Ecsit is required for Bmp signaling and mesoderm formation during mouse embryogenesis

Changchun Xiao,[1] Jae-hyuck Shim,[1,6] Michael Klüppel,[5,6] Samuel Shao-Min Zhang,[3,6] Chen Dong,[1,7] Richard A. Flavell,[1] Xin-Yuan Fu,[3] Jeffrey L. Wrana,[5] Brigid L.M. Hogan,[4] and Sankar Ghosh[1,2,8]

[1]Section of Immunobiology, [2]Department of Molecular Biophysics and Biochemistry, Howard Hughes Medical Institute, and [3]Department of Pathology, Yale University School of Medicine, New Haven, Connecticut 06520, USA; [4]Department of Cell Biology, Duke University Medical Center, Durham, North Carolina 27710, USA; [5]Programme in Molecular Biology and Cancer, Samuel Lunenfeld Research Institute, Mount Sinai Hospital, Toronto, Ontario M5G 1X5, Canada

Bone morphogenetic proteins (Bmps) are members of the transforming growth factor β (TGFβ) superfamily that play critical roles during mouse embryogenesis. Signaling by Bmp receptors is mediated mainly by Smad proteins. In this study, we show that a targeted null mutation of *Ecsit*, encoding a signaling intermediate of the Toll pathway, leads to reduced cell proliferation, altered epiblast patterning, impairment of mesoderm formation, and embryonic lethality at embryonic day 7.5 (E7.5), phenotypes that mimic the *Bmp receptor type1a* (*Bmpr1a*) null mutant. In addition, specific Bmp target gene expression is abolished in the absence of *Ecsit*. Biochemical analysis demonstrates that Ecsit associates constitutively with Smad4 and associates with Smad1 in a Bmp-inducible manner. Together with Smad1 and Smad4, Ecsit binds to the promoter of specific Bmp target genes. Finally, knock-down of *Ecsit* with *Ecsit*-specific short hairpin RNA inhibits both Bmp and Toll signaling. Therefore, these results show that Ecsit functions as an essential component in two important signal transduction pathways and establishes a novel role for Ecsit as a cofactor for Smad proteins in the Bmp signaling pathway.

[*Keywords*: NF-κ B; Toll-pathway; BMP signaling; Smads; mesoderm development; TGF β]

Supplemental material is available at http://www.genesdev.org.

Received August 20, 2003; revised version accepted October 10, 2003.

The transforming growth factor β (TGFβ) superfamily comprises a large number of secreted polypeptide factors, with >30 members in mammals and about a dozen in worms and flies. TGFβs control numerous cellular functions and regulate many developmental and homeostatic processes. However, a simple scheme lies at the core of all TGFβ signaling pathways. The receptor for TGFβ is a complex of two distinct transmembrane proteins, known as type I and type II receptors, with serine/threonine kinase activity within their cytoplasmic domains. Ligand binding to the type II receptor induces the association, phosphorylation, and activation of the type I receptor. The activated type I receptor then signals through the Smad family of signal transducers. Smad proteins can be divided into three classes: receptor-regulated Smads or R-Smads (Smad1, 2, 3, 5, 8); co-Smad (Smad4); and inhibitory Smads or I-Smads (Smad6 and 7). After stimulation, R-Smads are phosphorylated by type I receptors, detach from the receptor complex, associate with Smad4, and accumulate in the nucleus, where they regulate gene expression by interacting with various cofactors. Smad access to target genes and the recruitment of transcriptional coactivators or corepressors to these genes depend on cell-type-specific cofactors. Although many Smad cofactors have been identified for the TGFβ pathways, very few are known for the Bmp pathways (Wrana 2000; Shi and Massague 2003).

Genetic evidence has shown that Bmp4 plays pivotal roles in the gastrulation of mouse embryo, a process that lays down the future body plan (Lu et al. 2001). Bmp4 regulates the proliferation, survival, and patterning of the epiblast; the induction of primordial germ cell precursors; and formation of the mesoderm (Mishina et al. 1995; Winnier et al. 1995; Lawson et al. 1999). Bmp4 signals through Bmpr1a, a type I Bmp receptor, to induce the up-regulation of target genes including *Tlx2*, a homeobox gene that is a critical effector of Bmp signaling

[6]These authors contributed equally to this work.
[7]Present address: Department of Immunology, University of Washington, Box 357650, H466 Health Science Complex, Seattle, WA 98195-7650, USA.
[8]Corresponding author.
E-MAIL sankar.ghosh@yale.edu; FAX (203) 785-3855.
Article published online ahead of print. Article and publication date are at http://www.genesdev.org/cgi/doi/10.1101/gad.1145603.

(Tang et al. 1998). Mutant embryos deficient in *Bmp4*, *Bmpr1a*, or *Tlx2* are blocked at the beginning of gastrulation, and fail to form mesoderm. The mutant phenotype of Bmp4 varies on different genetic backgrounds, probably because of partial functional redundancy with Bmp2 and Bmp8b (Ying and Zhao 2001).

The Toll pathway was originally identified in *Drosophila* through genetic screens for mutants with embryo patterning deficiency. A key component of the pathway is the Toll receptor, whose engagement leads to the activation of transcription factors of the NF-κB family. Subsequent studies showed that the Toll pathway was also essential for host defense in the adult fly (Hoffmann and Reichhart 2002). The homologous family of Toll-like receptors (TLRs) in mammals also plays essential roles in innate immunity. The basic signal transduction pathway induced by the Toll receptors is homologous in *Drosophila* and mammals. Upon activation, TLRs recruit an adapter protein called MyD88, which subsequently recruits a serine–threonine kinase IRAK. IRAK binds to TRAF6, an adaptor protein of the tumor necrosis factor receptor-associated factor (TRAF) family. The assembly of this receptor complex activates IRAK, which undergoes autophosphorylation. Phosphorylated IRAK, together with TRAF6, detaches from the receptor complex and transduces the signal downstream, ultimately leading to activation of the IκB kinase (IKK) complex. The IKK complex phosphorylates IκB, leading to its ubiquitination and degradation. This process frees NF-κB and allows it to translocate into the nucleus, where it helps coordinate immune responses (Aderem and Ulevitch 2000). Two pathways have been proposed to bridge the signal from TRAF6 to the IKK complex. One pathway is through TAK1 and its associated adaptor proteins TAB1 and TAB2, whereas the other one goes through Ecsit and MEKK1 or other MAP3K kinases (Kopp et al. 1999; Deng et al. 2000; Wang et al. 2001). However, recent gene targeting results showed that TAB2 is not required for NF-κB activation in response to signaling through the Toll/IL-1 receptors (Sanjo et al. 2003).

Ecsit is a TRAF6-interacting protein that was discovered in a yeast two-hybrid screen using TRAF6 as bait (Kopp et al. 1999). The interaction between TRAF6 and Ecsit is conserved in *Drosophila*. Ecsit also interacts with MEKK1, an MAP3K kinase that can phosphorylate and activate the IKK complex. Expression of a dominant-negative mutant of Ecsit specifically blocks signaling from Toll and IL-1 receptors, but not from the TNF receptor. Therefore, Ecsit may transduce the signal from Toll receptors by bridging TRAF6 to the IKK complex (Kopp et al. 1999). To determine whether the TAK1/TAB1/TAB2 proteins can substitute for Ecsit in Toll signaling, and to further elucidate the physiological function of Ecsit, we deleted the *Ecsit* gene in embryonic stem cells and generated null mutant mice. *Ecsit*$^{-/-}$ mice died around embryonic day 7.5 (E7.5), and analysis of the mutant embryos revealed a striking similarity to the phenotype of mice lacking *Bmpr1a*. Further characterization showed that Ecsit is an obligatory intermediate in Bmp signaling that functions as a cofactor for Smad1/Smad4-dependent activation of specific Bmp target genes. In addition, ablation of Ecsit using shRNA results in the block of NF-κB activation by LPS, but not TNFα, demonstrating the specific involvement of Ecsit in Toll receptor signaling. Therefore, these studies show that Ecsit is an essential component in both Bmp and Toll signaling pathways and is required for early embryogenesis.

Results

Targeted disruption of Ecsit *causes early embryonic lethality*

Three different *Ecsit* cDNAs were cloned by screening mouse pre-B-cell and liver cDNA libraries. They are identical at their 5′-ends and differ at their 3′-ends (Kopp et al. 1999). Analysis of an *Ecsit* genomic DNA clone revealed that the three cDNAs, *Ecsit1*, *Ecsit2*, and *Ecsit3*, were derived from a single gene by alternative splicing (Fig. 1A). We generated a mutant allele of *Ecsit* by homologous recombination in embryonic stem (ES) cells, deleting a 6.1-kb fragment of the *Ecsit* gene that includes exons 2–8. The targeted allele has only exon 1 left, which ensures the inactivation of all three *Ecsit* spliced variants. Heterozygous mice carrying this mutation were generated from two independent ES clones (E142 and E147; see Materials and Methods) and were named after their corresponding clones. To avoid any unexpected effect of the neo cassette on neighboring genes, heterozygous male mice were bred with female *splicer* mice (Koni et al. 2001), which harbor a *Cre* transgene that is expressed in the eggs and deletes the floxed neo cassette at the one-cell stage. The offspring were screened for the targeted allele without the neo cassette and absence of the *Cre* transgene, because continuous expression of the Cre recombinase causes decreased cell growth, cytopathic effects, and chromosomal aberrations (Fig. 1; Silver and Livingston 2001). The resulting mouse lines were named E142/Neo$^-$ and E147/Neo$^-$, respectively. All four mouse lines, E142, E147, E142/Neo$^-$, and E147/Neo$^-$, exhibited the same mutant phenotype. Detailed analysis was mainly conducted with E142.

Mice heterozygous for the *Ecsit* mutation appeared morphologically normal and healthy and were fertile. There were no homozygous mutants among the progeny from interbreeding between heterozygotes of the four mouse lines (Supplemental Table 1), suggesting prenatal lethality of *Ecsit*$^{-/-}$ embryos. Histological analysis and genotyping of recovered embryos revealed that homozygous null embryos are smaller than normal from embryonic day 6.5 (E6.5), and no abnormal embryos could be recovered beyond E8.5 (Supplemental Table 1; data not shown). This showed that *Ecsit* is important for postimplantation development around the beginning of gastrulation.

Embryonic expression of Ecsit

A BLAST search of the NCBI est_mouse database (http://www.ncbi.nlm.nih.gov:80/BLAST/) found *Ecsit* ESTs in

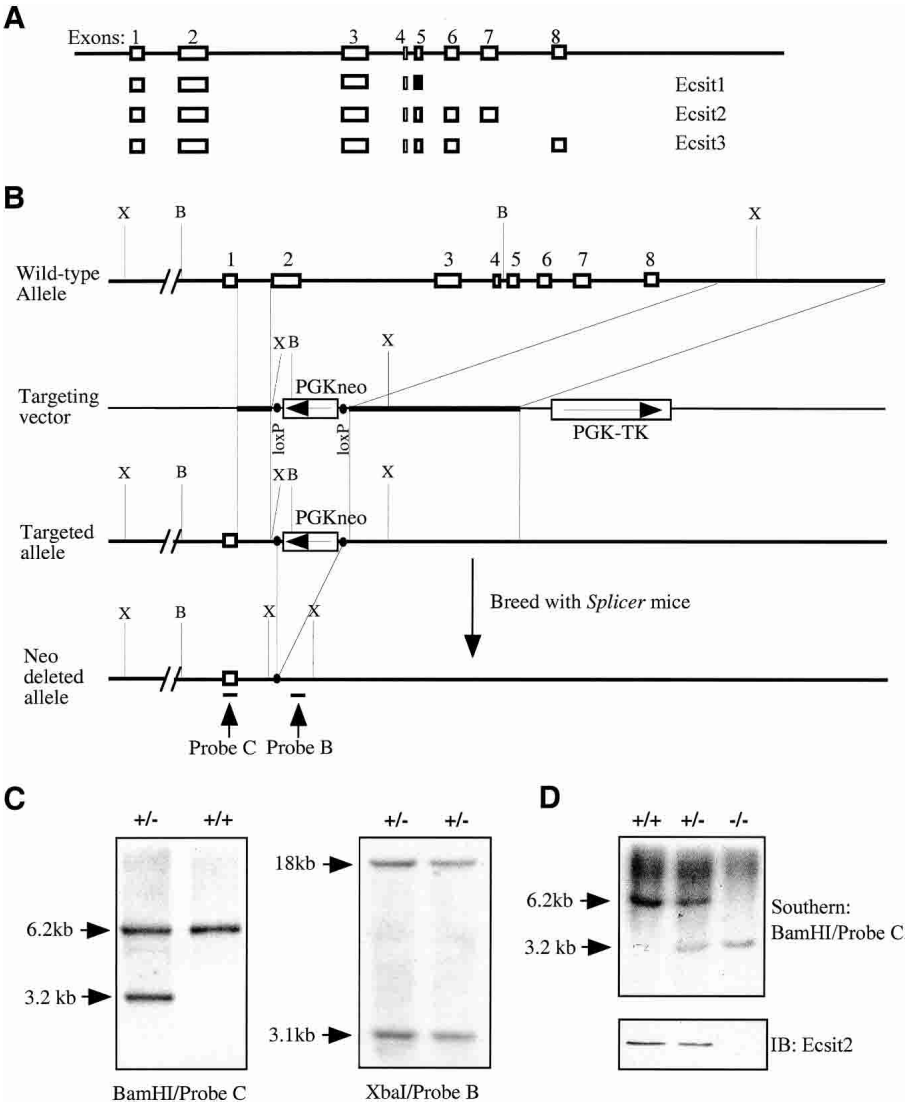

Figure 1. Generation of heterozygous and homozygous *Ecsit* mutant ES cell lines. (*A*) Gene structure of the *Ecsit* locus. In *Ecsit1*, exon 5 is used in different frame from that in *Ecsit2* and *Ecsit3*, as indicated by a black box in *Ecsit1* instead of the open boxes in *Ecsit2* and *Ecsit3*. (*B*) Targeting of the *Ecsit* locus. The targeting vector is described in Materials and Methods. Probe B and Probe C are indicated by bars. (B) BamHI; (X) XbaI. (*C*) Southern blot analysis of targeted ES clones. Using Probe C and BamHI digestion, the wild-type and targeted loci generate 6.2-kb and 3.2-kb bands, respectively. Using Probe B and XbaI digestion, the wild-type and targeted loci generate 18-kb and 3.1-kb bands, respectively. (*D*) Southern blot and Western blot analysis of $Ecsit^{-/-}$ ES clones. The Southern blot was done by using Probe C and BamHI digestion, and 40 μg of whole cell lysates for each clone was used in immunoblotting (IB).

ES cells and embryonic stages ranging from E6 to E19.5. The presence of Ecsit2 protein in ES cells was confirmed by immunoblotting (Fig. 1D). To determine the spatial expression pattern of *Ecsit* in early-stage embryos, whole-mount in situ hybridization was performed with probes specific to the alternatively spliced *Ecsit* variants, which correspond to the last exons of each spliced variant and their 3′-untranslated regions (3′-UTRs). Only *Ecsit2* expression was detected in embryos from E6.25 to E7.75 (Fig. 2). At E6.25, *Ecsit2* is expressed in the epiblast and the extraembryonic ectoderm (Fig. 2A,B). Between E7.0 and E7.75, *Ecsit2* is expressed mainly in the epiblast and in the embryonic mesoderm (Fig. 2D–K; data not shown). *Ecsit2* is also expressed in extraembryonic ectoderm and extraembryonic mesoderm (allantois and amnion) (Fig. 2G–K). At all the embryonic stages examined, *Ecsit2* expression in visceral endoderm and definitive endoderm is very weak, if it is expressed in these tissues at all.

Absence of mesoderm formation in Ecsit *mutant embryos*

Histological analysis combined with genotyping showed that at E6.5, *Ecsit* mutant embryos are smaller than normal ones (wild type or heterozygote). However, their egg

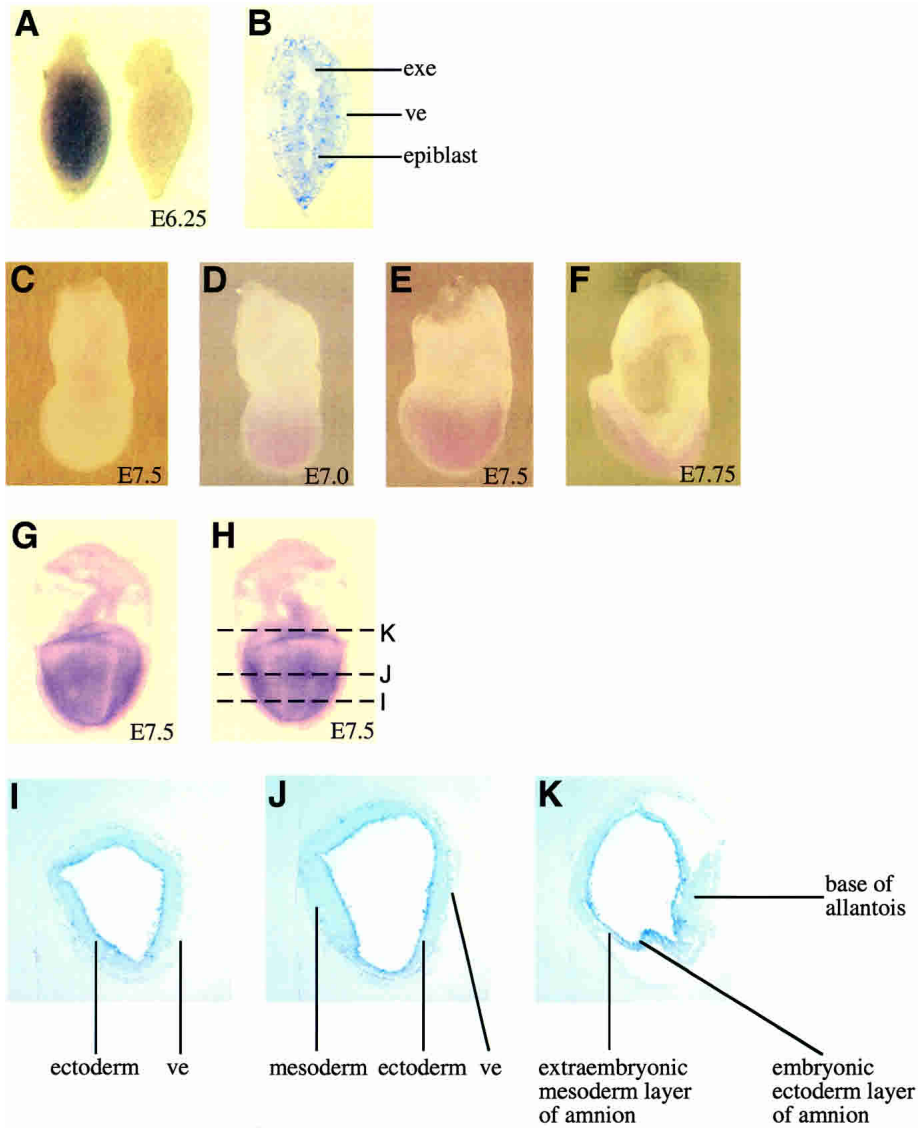

Figure 2. *Ecsit* expression in wild-type embryos as revealed by whole-mount in situ hybridization with *Ecsit2*-specific probes. (*A*) E6.25 embryos hybridized with (*left*) antisense probe or (*right*) sense probe. (*B*) Sagittal section of the left embryo in *A*. Note expression in epiblast and extraembryonic ectoderm. (*C*) E7.5 embryo hybridized with sense probe. (*D–F*) E7.0–E7.75 embryos hybridized with antisense probe. (*G*,*H*) Anterior (*G*) and posterior (*H*) view of an E7.5 embryo hybridized with antisense probe. (*I–K*) Cross-sections of the embryo in *H* along dashed lines. The color was developed for 200 h in *A*, 17 h in *C–F*, and 90 h in *G* and *H*. (exe) Extraembryonic ectoderm; (ve) visceral endoderm.

cylinder structure is quite normal, suggesting that cell proliferation is reduced (Fig. 3A,B). The difference between mutant and normal embryos is more striking at E7.5, when normal embryos have developed a distinctive primitive streak, mesoderm, head fold, amnion, chorion, and allantois (Fig. 3C). In contrast, all mutant embryos consist of an outer layer of visceral endoderm and an inner layer of epiblast and extraembryonic ectoderm. No obvious mesoderm layer was seen in all homozygous mutant embryos examined. However, at the putative proximal posterior region, a small group of cells (see asterisk in Fig. 3D) express *Brachyury*, a marker for laminating epiblast cells and the primitive streak (data not shown). These cells may represent nascent mesoderm. In the normal embryos, the epiblast consists of a single layer of cells. In the mutant embryos, however, the epiblast is thickened with multiple layers of cells (Fig. 3C–E). Some mutant embryos at E7.5 and most mutant embryos at E7.75 begin to degenerate and contain many blebbing cells (Fig. 3E). By E9.5, all mutant embryos are completely resorbed. Thus, mesoderm formation appears to be severely impaired in *Ecsit* mutant embryos.

Cell proliferation and apoptosis in the embryos were also examined by phospho-histone H3 (pH3) staining and TUNEL assay (Fig. 3F–H). There are four times more pH3-positive cells in the wild-type embryos than the

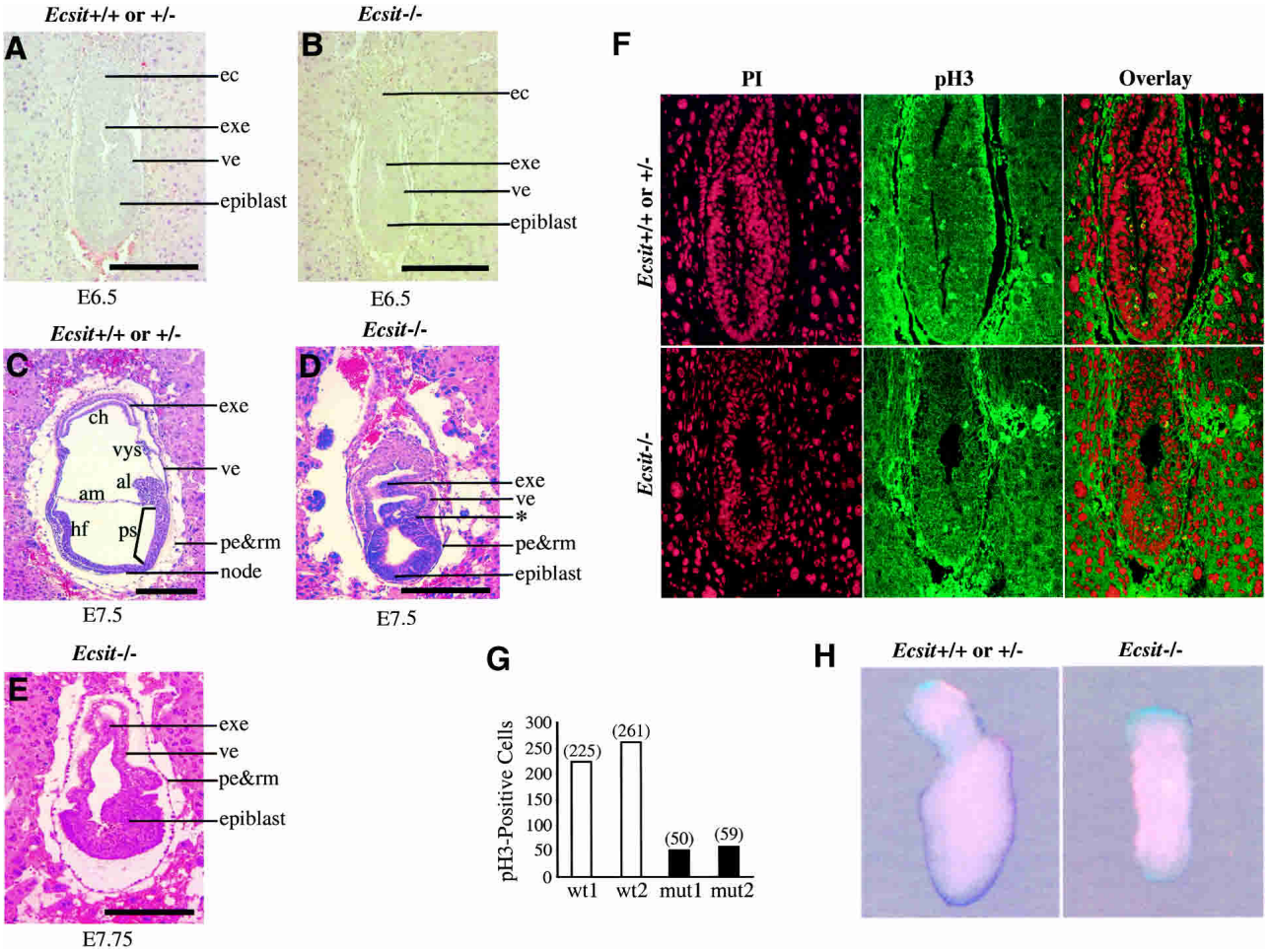

Figure 3. Histological analysis of *Ecsit* mutant embryos. (*A–E*) Wild-type (*Ecsit*$^{+/+}$) or heterozygous (*Ecsit*$^{+/-}$) embryos (*A*,*C*) and homozygous null (*Ecsit*$^{-/-}$) embryos (*B*,*D*,*E*) were embedded, sectioned, and stained with hematoxylin and eosin. Adjacent sections were hybridized with the *Ecsit2*-specific probe to genotype the embryos. Asterisk (*) in *D* marks delaminating epiblast. In all panels, anterior faces to the left when anterior–posterior orientation can be identified. (al) Allantois; (am) amnion; (ch) chorion; (ec) extraplacental cone; (exe) extraembryonic ectoderm; (hf) head fold; (pe&rm) parietal endoderm and Reichert's membrane; (ps) primitive streak; (ve) visceral endoderm; and (vys) visceral yolk sac. Bar, 250 µm. (*F*) E6.75 embryo sections were stained with anti-phosphohistone H3 antibody (pH3) and counterstained with propidium iodide (PI). (*G*) Numbers of pH3-positive cells in two wild-type (wt1 and wt2) and two *Ecsit*$^{-/-}$ mutant embryos (mut1 and mut2). (*H*) Whole-mount TUNEL staining of E6.75 embryos.

Ecsit$^{-/-}$ mutant embryos. TUNEL assays did not show any significant difference in apoptosis between wild-type and mutant embryos. Hence, these results demonstrate that cell proliferation is reduced in *Ecsit*-deficient embryos.

Epiblast patterning in Ecsit *mutant embryos*

Cell marking, tissue grafting, and gene targeting experiments demonstrate that interactions between the epiblast, extraembryonic ectoderm, and visceral endoderm are required for formation of the primitive streak and mesoderm (Lu et al. 2001). Because development of the mesoderm is impaired by the loss of *Ecsit*, the differentiation and morphology of all three tissue types were examined. We assessed cell migration, axis formation, and embryo patterning by examining a panel of genes showing regionalized expression in the embryo between E6.75 and E7.5, when *Ecsit* mutant embryos can be reliably distinguished. We analyzed the expression of *Cerberus-like* and *Brachyury* to assess the migration of distal visceral endoderm (DVE) and proximal epiblast, respectively. *Cerberus-like* is initially expressed in the DVE, which gradually moves to the anterior to become the anterior visceral endoderm (AVE; Stanley et al. 2000). *Brachyury* is first expressed in the proximal epiblast, and its expression then moves to the posterior, where it marks the primitive streak and nascent mesoderm (Beddington et al. 1992). We found that whereas both *Cerberus-like* and *Brachyury* were ultimately expressed in the correct location in *Ecsit* mutant embryos, their expression was delayed by 18–24 h (Fig. 4A,B; data not shown). It has been reported that a certain cell number must be reached to initiate gastrulation (Power and Tam

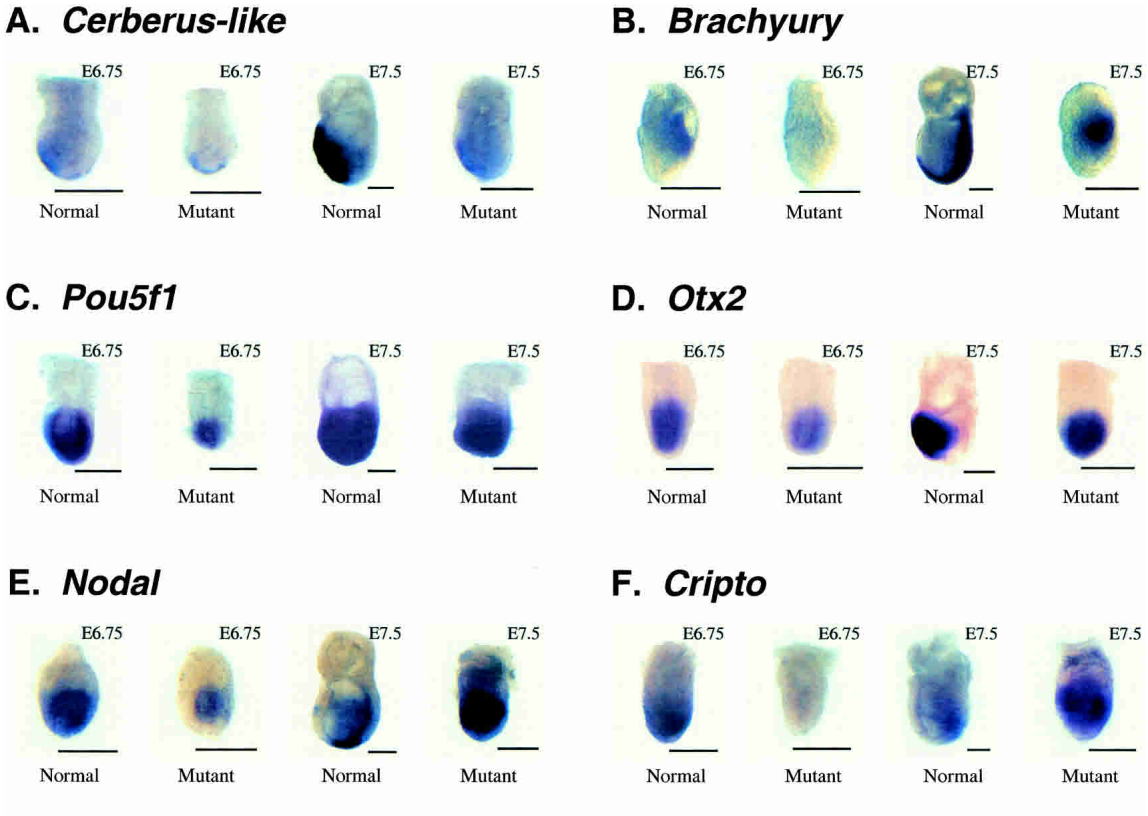

Figure 4. Expression of developmental markers in *Ecsit* mutant embryos. Whole-mount in situ hybridization with antisense probes of indicated genes. In all the panels, anterior faces to the left when anterior–posterior orientation can be identified. A minimum of five mutant embryos were assessed for each probe at each developmental time point. (Normal) $Ecsit^{+/+}$ or $Ecsit^{+/-}$; (Mutant) $Ecsit^{-/-}$. Bar, 300 μm.

1993). This delay was probably due to the reduced rate of proliferation of $Ecsit^{-/-}$ cells.

We also examined the expression of *Pou5f1* (*Oct3/4*), a member of the POU family transcription factors, which is strongly expressed by pluripotent epiblast cells and down-regulated as they differentiate (Rosner et al. 1990; Nichols et al. 1998). As shown in Figure 4C, *Pou5f1* is normally expressed in the epiblast of *Ecsit* mutant embryos from E6.75 to E7.5, demonstrating that these cells are pluripotent.

To further characterize patterning of the epiblast in *Ecsit* mutant embryos, we analyzed expression of *Otx2*, *Nodal*, and *Cripto*. *Otx2* is a bicoid-class homeobox gene, initially expressed throughout the epiblast and then gradually restricted to the anterior of the embryo in all three germ layers at the head fold stage (Simeone et al. 1993). Signals from the visceral endoderm surrounding the epiblast, and later from the primitive streak and nascent mesoderm, are thought to be involved in this restriction (Rhinn et al. 1998). Nodal is a TGFβ family member and plays a pivotal role in the patterning of pregastrulation embryos. Cripto is a member of the EGF-CFC gene family and functions as a coreceptor for Nodal. Both *Nodal* and *Cripto* are expressed throughout the epiblast at the egg cylinder stage in a proximal–distal graded pattern. Their expression in the anterior epiblast is then repressed by antagonists produced by the AVE, and is subsequently localized to the most posterior region of the embryo prior to primitive streak formation. Similar to *Cerberus-like* and *Brachyury*, the expression of *Nodal* and *Cripto* were delayed in mutant embryos. Strikingly, the expression of *Otx2*, *Nodal*, and *Cripto* remained uniform in the epiblast of mutant embryos at all embryonic stages examined, and did not become restricted to either anterior or posterior region at E7.5 (Fig. 4D–F; data not shown). This is probably because inhibitory signals are not generated in the visceral endoderm or these signals are not received by the epiblast in the absence of *Ecsit*.

Growth and differentiation potential of Ecsit$^{-/-}$ *ES cells*

The results presented above showed that epiblast cells in *Ecsit* mutant embryos have a decreased proliferation rate and abnormal patterning. We next assessed the growth and differentiation potential of $Ecsit^{-/-}$ ES cell lines, which were derived from the inner cell mass of blastocysts obtained by interbreeding *Ecsit* heterozygote mice. *Ecsit* deficiency in these cell lines was verified by Southern blotting and immunobotting using an antibody specific for Ecsit2 (Fig. 1D). To compare proliferation rate, equal numbers of cells of each genotype were plated on

feeder cells, or on gelatin, and cell numbers were counted every day for 4 d. As shown in Figure 5A, *Ecsit*$^{-/-}$ ES cells proliferated much more slowly than wild-type ES cells on feeder cells. More strikingly, *Ecsit*$^{-/-}$ ES cells completely stopped proliferation and some of them died when plated on gelatin, while wild-type ES cells still exhibited robust proliferation.

To determine the ability of the *Ecsit* mutant ES cells to differentiate into various cell types, we injected wild-type and mutant ES cells subcutaneously into nude mice. Then 7–9 wk after injection, the resulting teratomas were autopsied, weighed, fixed, and processed for histological analysis. Wild-type ES cells generated teratomas in 8 out of 19 mice injected, whereas *Ecsit* mutant ES cells generated teratomas in only 5 out of 19 mice injected (Supplemental Table 2). The most dramatic difference was observed in the sizes of the teratomas. Those derived from wild-type ES cells varied from 60 mg to 6.3 g, whereas those from mutant ES cells never exceeded 0.5 g (Supplemental Table 2; Fig. 5B). Histological analysis revealed that independent of the size of the tumor, wild-type ES cells generated well-differentiated tissues derived from all three germ layers, such as neural tissue and keratinized epithelium (from ectoderm); muscle, bone, bone marrow, and cartilage (from mesoderm); and adenoepithelium and intestinal adenoepithelium (from endoderm). In sharp contrast, *Ecsit* mutant ES cells generated poorly differentiated neural tissue, keratinized epithelium, and adenoepithelium-like tissue, suggesting that they were derived from either ectoderm or endoderm, but are deficient in mesodermal derivatives (Fig. 5C). In summary, the abilities of *Ecsit* mutant ES cells to differentiate and proliferate are limited.

Ecsit$^{-/-}$ *ES cells display impaired potential to contribute to embryonic tissues in diploid aggregation chimeras*

To analyze the developmental potential of *Ecsit*-deficient cells in more detail, we generated chimeric embryos in which the epiblast was composed of both ROSA26 wild-type cells and either *Ecsit*$^{+/+}$ or *Ecsit*$^{-/-}$ cells, whereas the extraembryonic and primitive endoderm lineages were composed of ROSA26 wild-type cells. For this we aggregated ROSA26 morulae, which were derived from matings of mice carrying the ROSA26 *lacZ* gene trap, with *Ecsit*$^{+/+}$ or *Ecsit*$^{-/-}$ ES cells. LacZ staining of the chimeric embryos allows the tracing of the contribution of ROSA26 and Ecsit cells to the various embryonic structures (Tremblay et al. 2000). Chimeric embryos were dissected at embryonic stages E8.5 (data not shown), E9.5, E12.5 (data not shown), and E14.5. Whereas *Ecsit*$^{+/+}$ cells in *Ecsit* $^{+/+}$ ↔ ROSA26 chimeras were able to contribute to all embryonic tissues at all embryonic stages tested, as indicated by various degrees of unstained portions of the embryos (Fig. 6A–C,H–J), *Ecsit*$^{-/-}$ ↔ ROSA26 chimeric embryos always displayed a dark blue stain (E8.5: $n = 13$; E9.5: $n = 14$; E12.5: $n = 11$; E14.5: $n = 9$), indicating that a large contribution of wild-type ROSA26 cells is required to compensate for the defects in *Ecsit*$^{-/-}$ cells and to allow the chimeric embryos to develop properly (Fig. 6D,K). Histological analysis of these *Ecsit*$^{-/-}$ ↔ ROSA26 chimeric embryos showed that at E9.5, *Ecsit*$^{-/-}$ cells have a very limited potential to contribute to embryonic structures (Fig. 6E–G). Some contribution of *Ecsit*$^{-/-}$ cells was seen in the neural tube (Fig. 6E), in the dermatome of the somites (Fig. 6F), and the myocardium of the developing heart (Fig. 6G), suggesting that *Ecsit*-deficient cells have residual potential to contribute to ectodermal and mesodermal derivatives.

Histological analysis of E14.5 chimeras showed that *Ecsit*$^{-/-}$ cells can efficiently contribute to neuroectoderm (Fig. 6L,M) and epidermis (Fig. 6M). Surprisingly, *Ecsit*$^{-/-}$ cells were also able to efficiently contribute to some mesodermal derivatives, like the dermis of the developing skin (Fig. 6M) and the mucosa in the gastrointestinal tract (Fig. 6O). Other mesodermal derivatives, like the myocardium of the heart (Fig. 6N), skeletal (Fig. 6M) and smooth muscle (Fig. 6O), and the lung mesenchyme (Fig. 6Q), showed only a very limited contribution of *Ecsit*$^{-/-}$ cells. Endodermal derivatives, like the gastrointestinal villi (Fig. 6O), the liver (Fig. 6P), and the lung epithelium (Fig. 6Q) also showed a limited contribution of *Ecsit*$^{-/-}$ cells. In summary, these diploid aggregation experiments showed a selective, impaired developmental potential for *Ecsit*-deficient cells, with a severe impairment in their ability to contribute to endodermal and some mesodermal derivatives, but an almost unaffected potential to contribute to most ectodermal and some mesodermal derivatives.

Ecsit *deficiency abolishes Bmp target gene expression*

The phenotypes of *Ecsit* mutant embryos and ES cells are reminiscent of those demonstrated by *Bmpr1a*-null mutants. In both cases, absence of the gene causes reduced epiblast cell proliferation, block of mesoderm formation, and embryonic lethality at the beginning of gastrulation. Analysis of teratomas derived from *Bmpr1a*$^{-/-}$ embryos and *Ecsit*$^{-/-}$ ES cells gave similar results (Table 1; Mishina et al. 1995). Therefore, we decided to examine the possible involvement of Ecsit in signaling by Bmpr1a.

The major ligand for Bmpr1a is Bmp4. *Bmp4* is first expressed in the inner cell mass of the blastocyst at very low level (Coucouvanis and Martin 1999). Subsequently, transcripts are detected throughout the uncavitated extraembryonic ectoderm at E5.5. By E6.0, just prior to primitive streak formation, the highest *Bmp4* expression is localized to the extraembryonic ectoderm region immediately adjacent to the epiblast. As gastrulation begins, *Bmp4* is also expressed in the newly formed extraembryonic mesoderm followed by the allantois and mesodermal components of the developing amnion, chorion, and visceral yolk sac (Lawson et al. 1999). *Bmpr1a* expression, on the other hand, can be detected throughout the epiblast and mesoderm at E6.75. It is then ubiquitously expressed, with higher expression in the epiblast, extraembryonic ectoderm, and extraembry-

onic mesoderm at E7.5. Expression of *Bmpr1a* in pregastrulation embryos is predicted but cannot be detected by in situ hybridization, probably because of the limited sensitivity of this method (Mishina et al. 1995). A normal pattern of *Bmp4* expression in *Ecsit* mutant embryos was seen in the embryonic stages examined (Fig. 7A; data not shown). A normal pattern of *Bmpr1a* expression in mutant embryos could also be detected from E7.25 onward (Fig. 7A; data not shown).

Next, we examined the expression of *Tlx2*, a known target gene for Bmp signaling. *Tlx2* is a homeobox gene (also known as *Hox11l1*), and its expression is induced by Bmp4 and mediated by Smad1 and Smad4. Targeted mutation of *Tlx2* leads to early embryonic lethality, caused by severe defects in mesoderm formation, a phenotype similar to *Bmpr1a* and *Ecsit* mutants (Table 1; Tang et al. 1998). By whole-mount in situ hybridization, *Tlx2* is first detected in E7.0 embryos in a broad domain that correlates with the epiblast, the extraembryonic ectoderm, and the primitive streak. At E7.5, *Tlx2* expression is only seen in the extreme posterior end of the primitive streak and in two symmetrical stripes that extend laterally on either side of the streak (Tang et al. 1998). Although the *Tlx2* expression pattern in normal embryos was consistent with prior reports, there was no *Tlx2* expression detected in *Ecsit* mutant embryos (Fig. 7A). Hence, whereas both *Bmp4* and *Bmpr1a* were expressed at their correct locations, the expression of the Bmp target gene *Tlx2* was undetectable in *Ecsit* mutant embryos. Therefore, this result strongly suggests that signaling through the Bmp receptor is disrupted in the absence of *Ecsit*.

Ecsit is indispensable for Bmp signaling

The early embryonic lethality of *Ecsit* mutant embryos prevented us from obtaining mutant cells that could be used to study Bmp signaling. We therefore used small interfering RNA (siRNA) technology to directly examine the role of Ecsit in the Bmp signaling pathway. Two 19-nt target sequences of the *Ecsit* gene (Sh1 and Sh2) were cloned into a pBluescript KS+ vector along with an H1-RNA promoter, which directs synthesis of short hairpin RNA (shRNA), and the resulting transcript can be converted into an siRNA capable of knocking down target gene expression (Brummelkamp et al. 2002). Transient transfection of Sh2 in COS1 cells resulted in a dramatic reduction of the transiently expressed Ecsit2 protein, whereas Sh1 and the empty vector were inactive in this assay (Fig. 7B). Next, we tested the effect of reducing Ecsit protein level in P19 cells, an embryonic carcinoma cell line derived from pregastrulation mouse embryos (McBurney and Rogers 1982). P19 cells can be induced to differentiate into derivatives of the three germ layers in response to Bmps and activins (Vidricaire et al. 1994). Tlx2-luc is a reporter construct with the luciferase gene under the control of the 1.6-kb *Tlx2* promoter (Tang et al. 1998). As shown in Figure 7B, transient transfection of Sh2 into P19 cells significantly reduced Bmp4-induced *Tlx2* promoter activity in a dose-dependent manner, whereas Sh1, the control shRNA that does not affect Ecsit protein level in COS1 transient transfection assays, had no effect on *Tlx2* promoter activity. Therefore these results strongly suggest that Ecsit is an essential intermediate in Bmp signaling.

Ecsit functions as a Smad cofactor

Signaling through Bmpr1a is primarily mediated by Smad1 and Smad4. Upon receptor activation, Bmpr1a phosphorylates Smad1, which then forms a complex with Smad4. The Smad1:Smad4 complex accumulates in the nucleus, where it regulates the expression of target genes (Shi and Massague 2003). Because Ecsit2 localizes to both the cytoplasm and the nucleus (data not shown), it is possible that Ecsit might regulate Bmp signaling in either subcellular location.

We began our analysis of the role of Ecsit in Bmp signaling by testing whether endogenous Ecsit2 interacts with endogenous Smads in Bmp-responsive P19 cells. We focused on Ecsit2 because it is the only Ecsit isoform expressed in P19 cells (and in the embryonic stages E6.25–E7.75; data not shown). The level of endogenous Ecsit2 protein did not change significantly upon Bmp4 stimulation of P19 cells (Fig. 7C). Remarkably, Ecsit2 could be coprecipitated with Smad4 from both treated and untreated cells, while Smad1 coprecipitated with Ecsit2 only after Bmp4 treatment (Fig. 7C). This suggests that although Ecsit2 appears to constitutively associate with Smad4, it associates with Smad1 in a Bmp-inducible manner. This result also suggests that association of Ecsit2 with Smad1 is dependent on phosphorylation of Smad1 by ligand-activated Bmpr1a.

It has been previously demonstrated that the Smad1:Smad4 complex binds to DNA directly, raising the possibility that Ecsit also binds to DNA. To test this possibility, we decided to use chromatin-immunoprecipitation assays (ChIP) to examine whether Ecsit is associated to a Bmp-responsive promoter. We decided to map the Bmp-response element in the *Tlx2* promoter

Figure 5. *Escit*$^{-/-}$ ES cells are deficient in both proliferation and differentiation. (*A*) Growth curve of wild-type (*Ecsit*$^{+/+}$) and mutant (*Ecsit*$^{-/-}$) ES cells on feeder cells (feeders) and gelatin-coated plates (gelatin). Assays were done with two wild-type, one heterozygous, and six mutant ES cell lines; results from one wild-type and one mutant cell line are presented. The heterozygous cell line gave the same result as the wild-type cell lines. (*B*) Wild-type (*Ecsit*$^{+/+}$) and mutant (*Ecsit*$^{-/-}$) ES cells were injected subcutaneously into nude mice. The mice were photographed 7 wk after injection. (*C*) Histological analysis of teratomas derived from ES cells. Tissues arising from wild-type ES cells are shown in *a, b, d, e, g,* and *h*. Tissues arising from mutant ES cells are shown in *c, f,* and *i*. (ae) Adenoepithelium; (ael) adenoepithelium-like tissue; (bo) bone; (bm) bone marrow; (ca) cartilage; (iae) intestine adenoepithelium; (ke) keratinized epithelium; (mu) muscle; (ne) neural tissue; (nel) neural epithelium-like tissue; and (pc) Paneth cells.

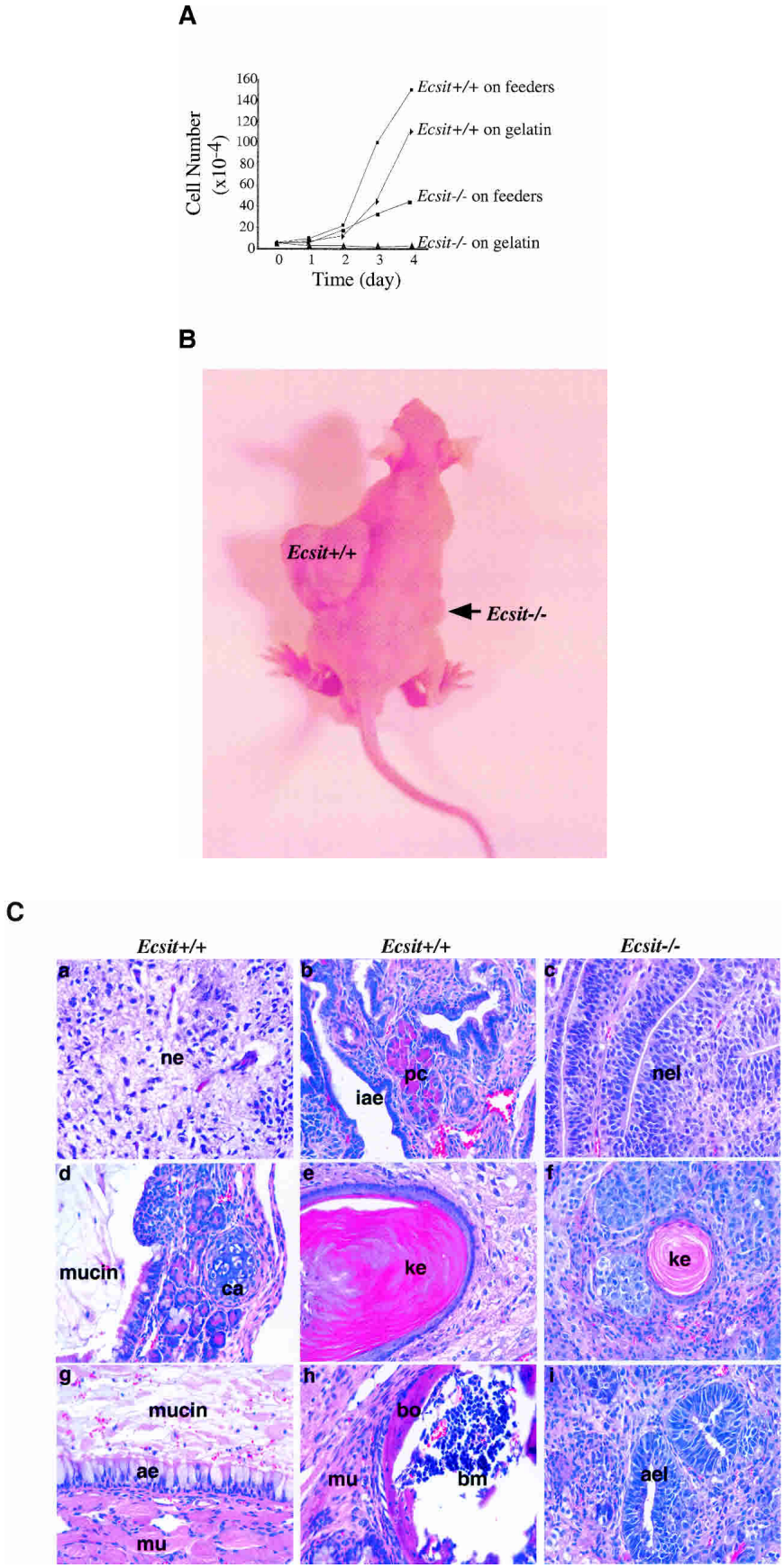

Figure 5. (*See facing page for legend.*)

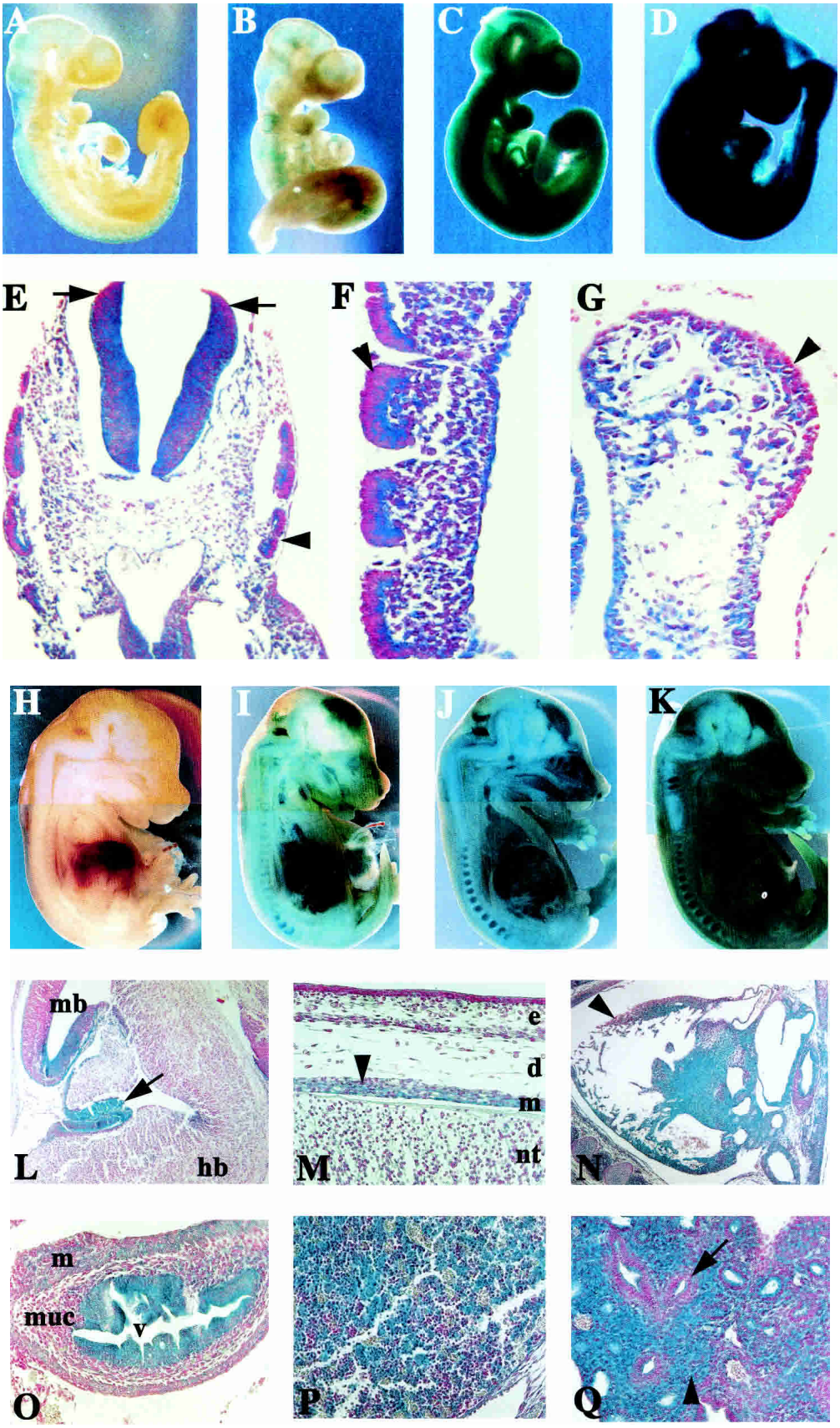

Figure 6. (*See facing page for legend.*)

Table 1. *Comparison of phenotypes of* Bmpr1a, Ecsit, *and* Tlx2 *mutants*

Bmpr1a$^{-/-}$[a]	*Ecsit*$^{-/-}$	*Tlx2*$^{-/-}$[b]
1. Embryonic lethality at E6.5–E7.5	Embryonic lethality at E6.5–E7.5	Embryonic lethality at E7.0–E7.5
2. No Brachyury-expressing mesoderm by E7.0 (E7.5 embryos not examined)	Little Brachyury-expressing mesoderm at E7.5	Little Brachyury-expressing mesoderm at E7.0–E7.5
3. Mutant embryos smaller than wild type from E6.5–E7.0	Mutant embryos smaller than wild type from E6.5–E7.0	Mutant embryos smaller than wild type from E7.0–E7.5
4. The epiblast/ectoderm is multilayered.	The epiblast/ectoderm is multilayered	The epiblast/ectoderm is multilayered
5. Proliferation of mutant epiblast cells decreased by E6.5, as determined by BrdU incorporation	Proliferation of mutant cells decreased, as determined by ES cell growth curve and embryo pH3 staining	N.R.
6. Proliferation and differentiation abilities of cells derived from E6.5 mutant embryos are limited, when transplanted into testes and grown as teratomas	Proliferation and differentiation abilities of mutant ES cells are limited, when injected into nude mice and grown as teratomas. This is also shown by chimera analysis.	N.R.

[a]Mishina et al. 1995.
[b]Tang et al. 1998.
N.R., not reported.

because *Tlx2* is a well-characterized target gene for Bmp signaling and it functions at the embryonic stage when Ecsit is essential for embryo development. A series of 5′-end progressive deletions of the promoter were generated and placed upstream of a luciferase reporter gene. The promoter activity of these constructs was tested in a luciferase reporter assay. As shown in Figure7D, the 5′ 531-bp fragment (–1602/–1072) was essential for Bmp-responsiveness. The 531-bp promoter fragment was further dissected, and we found that the –1443/–1072 portion contained the Bmp-response element (Fig. 7D). Using this Bmp-responsive element, we performed chromatin immunoprecipitation experiments. As shown in Figure 7E, Smad1, Smad4, and Ecsit2 antibodies were able to precipitate the Bmp-response element of the *Tlx2* promoter (*Tlx2* BRE), but were unable to precipitate a 3′-region of the *Tlx2* gene (*Tlx2* 3′). Remarkably, Smad4 and Ecsit2 associate with the *Tlx2* promoter before cells are exposed to Bmp4, and treatment with Bmp4 enhances Smad4 binding but weakens Ecsit2 binding. This suggests that although the Ecsit2:Smad4 complex binds to the Bmp-response element of the *Tlx2* promoter in unstimulated cells, in the absence of Bmp4 stimulation, it is unable to promote transcription. Upon Bmp4 stimulation, phosphorylated Smad1 probably joins this complex, and the tripartite Smad1:Smad4:Ecsit2 complex is then able to drive transcription. The change of binding efficiency of Smad4 and Ecsit2 to the *Tlx2* BRE is probably due to change in local chromatin structure following Bmp4 treatment, and/or the binding of Smad1 to this region.

Ecsit is also an essential component of the Toll pathway

Ecsit was originally discovered as a signaling intermediate in the Toll/IL-1R pathway, but not the TNFα pathway. The extremely early embryonic lethality of the *Ecsit*-deficient embryos prevented us from obtaining *Ecsit*$^{-/-}$ cells suitable for analyzing Toll/IL-1R signaling. Therefore, we used the Ecsit shRNAs to knock down Ecsit in a macrophage cell line, Raw 264.1, to assess its

Figure 6. *Ecsit*$^{-/-}$ ES cells are compromised in their ability to contribute to mesodermal and endodermal derivatives in diploid aggregation chimeras. ROSA26 morulae were aggregated with either (*A–C*,*H–J*) *Ecsit*$^{+/+}$ ES cells (*Ecsit*$^{+/+}$ ↔ ROSA26) or (*D–G*,*K–Q*) *Ecsit*$^{-/-}$ ES cells (*Ecsit*$^{-/-}$ ↔ ROSA26). Embryos were dissected at either (*A–G*) E9.5 or (*H–Q*) E14.5, and the whole-mount embryos were stained for β-galactosidase, resulting in blue staining of ROSA26 cells. Counterstaining leads to red staining of Ecsit cells. Whereas *Ecsit*$^{+/+}$ ES cells were able to contribute to the embryos to various degrees at E9.5 (*A*: 100% contribution; *B*: ~70% contribution; *C*: <20% contribution), embryos resulting from aggregations of *Ecsit*$^{-/-}$ ES cells to ROSA26 morulae always showed very little contribution of the *Ecsit*$^{-/-}$ cells at E9.5 (*D*; $n = 14$). Sectioning of these *Ecsit*$^{-/-}$ ↔ ROSA26 chimeric embryos showed a large contribution of blue-stained ROSA26 cells in almost all tissues. *Ecsit*$^{-/-}$ cells were able to contribute in a limited fashion to the neural tube (arrows in *E*), the dermatome of the somites (arrowheads in *E* and *F*), and the myocardium of the heart (arrowhead in *G*). At E14.5, *Ecsit*$^{+/+}$ cells were again able to contribute to the chimeric embryos to various degrees (*H–J*), whereas *Ecsit*$^{-/-}$ ↔ ROSA26 chimeras always stained dark blue (*K*; $n = 9$). (*L–Q*) Sections of *Ecsit*$^{-/-}$ ↔ ROSA26 chimeras. (*L*) *Ecsit*$^{-/-}$ cells can efficiently contribute to neuroectoderm. (mb) Midbrain; (hb) hindrain; (arrow) choroid plexus. (*M*) *Ecsit*$^{-/-}$ cells contribute efficiently to the neural tube (nt), the dermis (d), and epidermis (e), but not muscle tissue (m). (*N*) Limited contribution of *Ecsit*$^{-/-}$ cells to heart tissue (arrowhead). (*O*) Low contribution of *Ecsit*$^{-/-}$ cells to the villi (v) and smooth muscle (m) and efficient contribution to the mucosa (muc) in the gastrointestinal tract. (*P*) Limited contribution of *Ecsit*$^{-/-}$ cells to embryonic liver. (*Q*) Very limited contribution of *Ecsit*$^{-/-}$ cells to lung mesenchyme (arrowhead) and efficient contribution to lung epithelium (arrow).

function in the Toll pathway. Knock-down of Ecsit in these cells led to a drastic inhibition of LPS-induced NF-κB activity. In contrast, the control shRNA that does not affect Ecsit protein level had no effect on LPS-induced activation of NF-κB in Raw cells (Fig. 8A). More remarkably, the knock-down of Ecsit had very little effect on TNFα-induced NF-κB activation (Fig. 8B). Therefore, this result supports our prior findings that Ecsit is an exclusive intermediary in the Toll pathway, but not in the TNFα pathway.

Discussion

Ecsit is an essential Smad cofactor of Bmp signaling

The results of this study have revealed an unanticipated function of the mammalian Ecsit protein in Bmp signaling pathways that lead to the activation of specific Bmp-responsive promoters. Ecsit functions in association with Smad proteins and is constitutively associated with Smad4 in unstimulated cells, but only associates with Smad1 in cells stimulated with Bmp. Moreover, deletion of *Ecsit* prevents expression of specific Bmp target genes and blocks embryonic development at the beginning of gastrulation, strongly suggesting that Ecsit is an obligatory component of Bmp signaling pathways controlling the activity of specific Bmp-responsive target genes.

An important means of regulating Smad activity is through the association of R-Smad:Smad4 complexes with specific cofactors. Smads can bind DNA directly, but with low affinity and specificity, and they rely on these cofactors to achieve activation of specific target genes. These cofactors include transcription factors, DNA-binding proteins without intrinsic transactivation activity, histone acetylase/deacetylace, and other proteins. The first identified Smad DNA-binding partner was FAST (Foxh1 in mouse), a winged helix forkhead transcription factor, which regulates activin-dependent expression of the *mix.2* gene in *Xenopus* and the *goosecoid* gene in mouse. FAST by itself can bind to the promoters of these genes without activating their expression. Upon activin stimulation, Smad2 and Smad4 form complexes with FAST and transcription is strongly activated (Wrana 2000). OAZ, a 30-zinc finger protein, is another Smad partner protein shown recently to function in the Bmp pathway. OAZ associates with Smad1 and Smad4 in response to Bmp2, forming a complex that activates transcription of *Xvent-2*, a homeobox regulator of *Xenopus* mesoderm and neural development (Hata et al. 2000). Intriguingly, OAZ was also implicated as a transcriptional partner of Olf/EBF in olfactory epithelium and lymphocyte development. OAZ interacts with Smads and Olf/EBF through different clusters of its zinc fingers. Smads and Olf/EBF act antagonistically in their ability to share OAZ as a DNA-binding partner. In doing so, OAZ functions to integrate signals from multiple pathways to regulate patterning during *Xenopus* development. So far, many Smad cofactors have been identified for the TGFβ/activin pathways, but few are known for the Bmp pathways. Furthermore, Smad cofactors important for the Bmp signaling in early stage of mouse embryo development are unknown. The identification of Ecsit as an Smad cofactor essential for this stage of mouse embryo development helps fill this gap. The kinetics of Ecsit interaction with Smad1 and Smad4 is very similar to that of FAST and OAZ with their corresponding Smad proteins, and based on our results, we propose a similar model for the function of Ecsit in Bmp signaling. In resting cells, Ecsit binds constitutively to Smad4 and the Ecsit:Smad4 complex binds to promoters of certain target genes, without activating transcription. When the Bmp pathway is activated, phosphorylated Smad1 translocates to the nucleus and binds to the Ecsit:Smad4 complex to form a higher-order complex containing Ecsit, Smad1, and Smad4. Assembly of this complex appears to be necessary for transcription to be initiated from the promoters of appropriate Bmp-target genes (Fig. 9). Because Smad4 participates in all TGFβ superfamily pathways and Ecsit2 constitutively interacts with

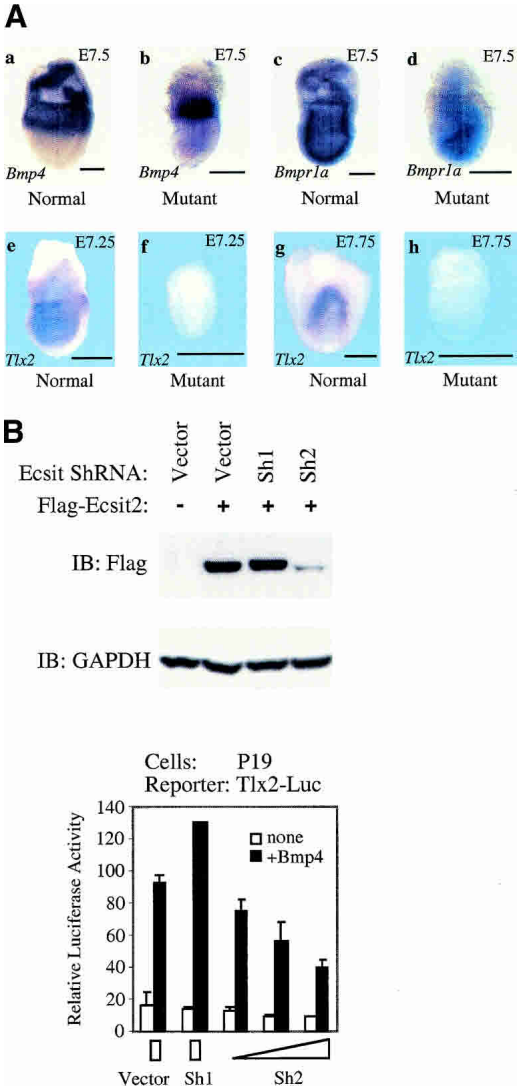

Figure 7. (*See facing page for legend.*)

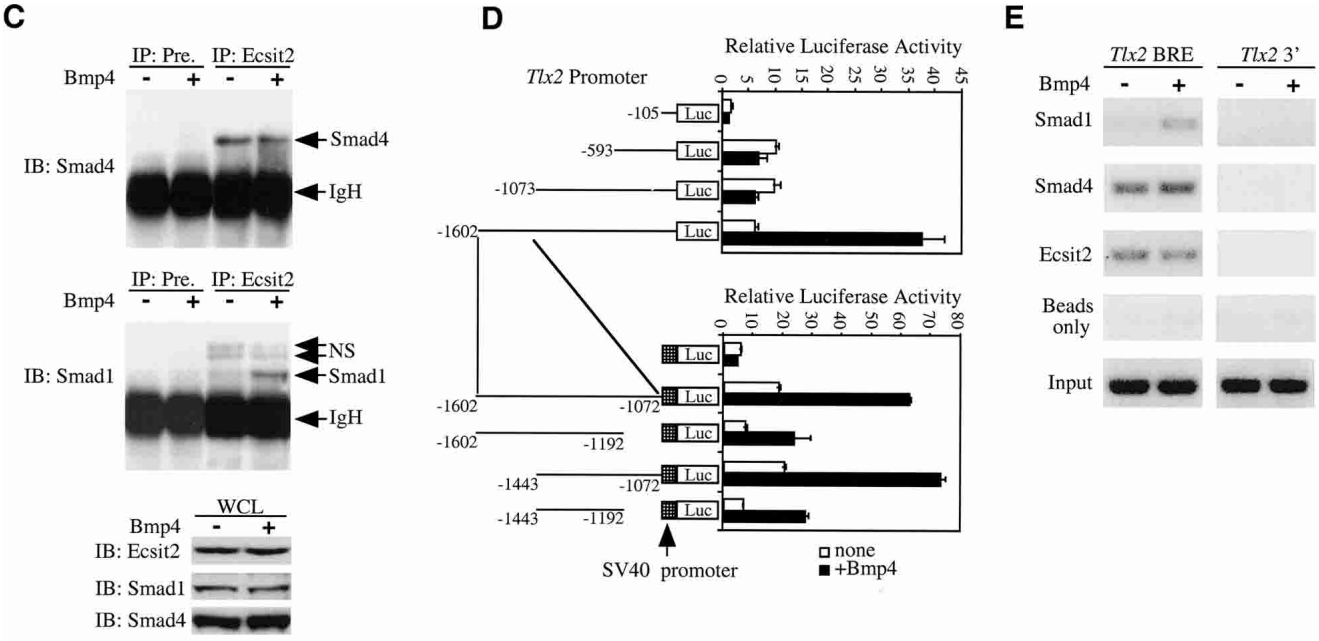

Figure 7. Ecsit is essential for Bmp signaling. (*A*) Expression of *Bmp4*, *Bmpr1a*, and *Tlx2* in mutant embryos. Whole-mount in situ hybridization was done with antisense probes of indicated genes. Anterior faces left when anterior–posterior orientation can be identified in all panels except *g*, in which the posterior view is presented. Bar, 300 µm. (*B*) Ecsit ShRNA inhibits Bmp signaling. (*Upper* panel) Flag-Ecsit2 and Ecsit ShRNAs were cotransfected into COS1 cells at 1:7 ratio. Then, 48 h after transfection, cell were lysed and whole cell lysates were immunoblotted with antibodies specific for Flag and GAPDH. (*Lower* panel) Luciferase reporters containing the promoter region of the mouse *Tlx2* gene (Tlx2-Luc) were cotransfected with pBluescript KS+ (Vector, 1:7 ratio), Sh1 (1:7), or Sh2 (1:1, 1:3, 1:7) into P19 cells. Then, 48 h after transfection, cells were treated (black bars) or untreated (open bars) with 20 ng/mL Bmp4 for 15 h prior to lysis and then analyzed for luciferase activity. (*C*) Ecsit associates with Smad1 and Smad4. P19 cells were untreated or treated with 20 ng/mL Bmp4 for 30 min. Proteins precipitated (IP) with Ecsit2-specific antibody or preimmune serum (Pre.) were immunoblotted (IB) with antibodies specific for Smad1 and Smad4. The same amount of whole cell lysates (WCL) from each sample was immunoblotted with Ecsit2-, Smad1-, and Smad4-specific antibodies. (NS) Nonspecific; (IgH) immunoglobulin heavy chain. (*D*) *Tlx2* promoter analysis. pGL2-Basic containing 5′ deletions of the *Tlx2* promoter or pGL2-Promoter containing fragments spanning the Bmp-response element were transfected into P19. Then, 12 h after transfection, cells were treated with 20 ng/mL Bmp4 for 15 h prior to lysis and analyzed for luciferase activity. (*E*) Ecsit 2, Smad1, and Smad4 bind to the *Tlx2* promoter. Soluble chromatin was prepared from P19 cells untreated or treated with 20 ng/mL Bmp4 for 30 min and immunoprecipitated with specific antibodies. The final DNA extractions were amplified using primers that cover the *Tlx2* BRE and a 3′-region of the *Tlx2* gene (4504/4759; *Tlx2* 3′).

Smad4, it is possible that Ecsit2 might also play a role in the signaling from other TGFβ family members.

Ecsit, epiblast proliferation, and mesoderm formation

Our results show that *Ecsit* is necessary for both epiblast proliferation and mesoderm formation. It is possible that the absence of mesoderm formation is a secondary defect caused by the decreased proliferation rate of epiblast cells. However, histological analysis of teratomas derived from ES cells suggests that there is no direct correlation between proliferation and differentiation. Regardless of size, all wild-type ES cell-derived teratomas contain mesoderm-derived tissue, which was severely reduced in all *Ecsit*$^{-/-}$ ES cell-derived teratomas. The impairment of *Ecsit* mutant ES cells to differentiate into mesoderm-derived tissue therefore demonstrates that *Ecsit* is directly involved in the production of or response to mesoderm-inducing signals.

Our diploid aggregation chimera analysis further supports the proposed role for Ecsit in mesoderm formation. This analysis, however, also clearly showed that whereas Ecsit is required for the development of some mesodermal derivatives, like cardiac, skeletal, and smooth muscle as well as lung mesenchyme, other mesodermal derivatives, including the dermis and the gut mucosa, seem not to require functional Ecsit protein for proper development. Moreover, although Ecsit appears to be required for the proper development of most endodermal derivatives, ectodermal lineages seem not to require functional Ecsit. Therefore, Ecsit is required for the development of a subset of endodermal and mesodermal lineages during embryogenesis.

Comparisons of phenotypes of embryos deficient of *Bmpr1a*, *Ecsit*, and *Tlx2* reveal a genetic pathway: Bmpr1a → (Smad1/4) Ecsit → Tlx2, with the *Bmpr1a* mutant phenotype the most severe and the *Tlx2* mutant phenotype the least severe (Table 1). Both *Bmpr1a* and *Ecsit* mutant embryos become smaller than wild type at E6.5–E7.0, whereas *Tlx2* mutant embryos do not become

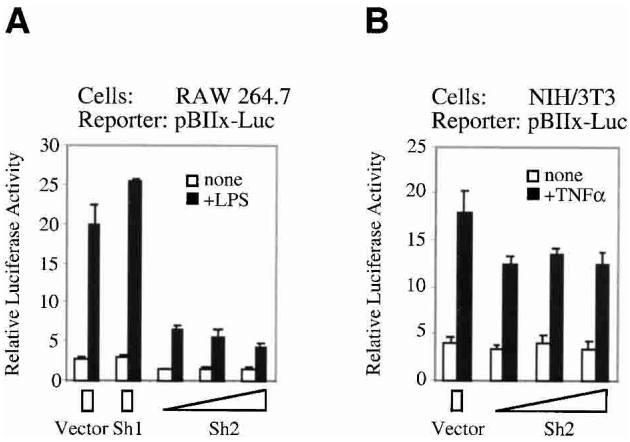

Figure 8. Ecsit ShRNA inhibits Toll but not TNF signaling. Luciferase reporters containing two NF-κB binding sites (pBIIx-Luc) were cotransfected with pBluescript KS+ (Vector, 1:7 ratio), Sh1 (1:7), or Sh2 (1:1, 1:3, 1:7) into RAW 264.7 (*A*) or NIH/3T3 (*B*) cells. Then, 48 h after transfection, cells were treated (black bars) or untreated (open bars) with 100 ng/mL LPS (*A*) or 25 ng/mL TNFα (*B*) for 4 h prior to lysis and analyzed for luciferase activity.

smaller than wild type until E7.0–E7.5. There are no *Brachyury*-expressing cells in *Bmpr1a* mutant embryos, whereas *Brachyury*-expressing cells appear at E7.25–E7.5 in *Ecsit* mutant embryos and at E7.0 in *Tlx2* mutant embryos. The difference in severity of these mutant phenotypes suggests that Ecsit regulates only a subset of target genes activated by Bmpr1a and *Tlx2* is one of them.

Taken together, it appears that the *Ecsit* mutant phenotype is mainly due to deficiency in the Bmp signaling pathway. The function of Bmp signaling in promoting epiblast proliferation and inducing mesoderm formation has been well established (Mishina et al. 1995; Winnier et al. 1995). However, it remains unclear how Bmp signaling carries out these functions. One possibility is that Bmp signaling is necessary to convey signals from extraembryonic tissues that are crucial for establishing the anterior–posterior axis in the epiblast (Mishina et al. 1995). Therefore, *Ecsit* deficiency could lead to lack of proper signals from extraembryonic tissues, or incompetence of epiblast cells to respond to these signals, or both.

Interplay of Toll pathway and TGFβ/Bmp pathways

Cross-talk between the Toll pathway and TGFβ/Bmp pathways has been well documented in prior studies. At the syncytial stage of *Drosophila* embryo development, the expression of *decapentaplegic* (*Dpp*), a close homolog of mammalian *Bmp4* and a morphogen that specifies the dorsal fate of the *Drosophila* embryo, is under tight regulation by the Toll pathway. Dorsal, activated by Toll, binds directly to multiple sites in the *Dpp* gene and represses its expression in the ventral domain of the embryo (Huang et al. 1993). The interaction between the Toll and Dpp pathways establishes the dorsoventral axis of the *Drosophila* embryo (Wharton et al. 1993).

There is also considerable evidence that the Toll and TGFβ pathways antagonize each other in the mammalian immune response. Whereas Toll-like receptors (TLRs), which recognize signature structures of various pathogens, induce inflammation and subsequently activate the adaptive immune responses, TGFβ generally plays an anti-inflammatory and immunosuppressive role (Letterio and Roberts 1997; Aderem and Ulevitch 2000). Many important target genes of proinflammatory stimuli contain binding sites for both NF-κB and Smads in their promoters, which can be activated or repressed by the Toll pathway and the TGFβ pathway, respectively (Geiser et al. 1993; Vodovotz et al. 1996). An additional means through which antagonism between these pathways is mediated is through inhibitory Smads. Lipopolysaccharide (LPS) up-regulates Smad7 expression through the TLR4-NF-κB pathway. Smad7 then suppresses TGFβ by its direct interaction with the TGFβ type I receptor and blocking TGFβ-induced Smad phosphorylation (Bitzer et al. 2000).

Our present study adds a potential new mechanism for cross-regulating the Toll and Bmp pathways. By func-

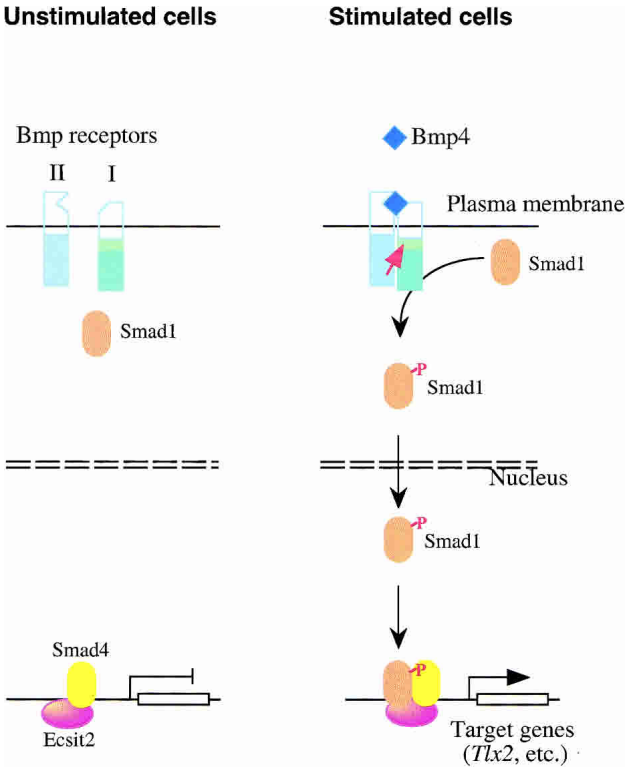

Figure 9. Ecsit is a cofactor for Smad proteins in Bmp signaling. In unstimulated cells, Ecsit2 and Smad4 bind to the promoters of target genes, but are not able to drive transcription. Upon Bmp stimulation, Smad1 is phosphorylated, translocates to the nucleus, and forms a complex with Smad4 and Ecsit2 on the target gene promoters, which is then able to drive transcription. The red arrow indicates phosphorylation of the type I receptor by the type II receptor. (P) Phosphate group.

tioning as an essential component in both pathways, Ecsit might help determine which pathway functions at any one time. Our earlier studies had indicated that Ecsit is potentially modified during Toll signaling (Kopp et al. 1999). It is possible that modified Ecsit might not function in the Bmp pathway and would therefore inhibit Bmp/TGFβ signaling. Alternatively, Bmp/TGFβ signaling might suppress Toll signaling by sequestering Ecsit in nuclear Smad complexes. Determining the exact mechanism by which Ecsit mediates cross-talk between these pathways will require detailed biochemical analysis of Ecsit function in response to signaling through both pathways, and these studies will be significantly facilitated by the future availability of conditional knockouts of *Ecsit*.

Materials and methods

Targeting Ecsit *and generation of* Ecsit$^{+/-}$ *mice and* Ecsit$^{-/-}$ *ES cells*

One *Ecsit* genomic clone was isolated from a 129/SvJ mouse genomic library (Stratagene). The targeting vector consists of a 1.3-kb 5′ homology region and a 4.2-kb 3′ homology region. A loxP-PGKneo-loxP cassette was inserted between the two regions, and a PGK-TK cassette was placed at the end of the 3′ homology region, resulting in a vector designed to delete exons 2–8 of *Ecsit*. Linearized targeting vector was electroporated into TC1 ES cells. Clones resistant to G418 and gancyclovir were selected, and homologous recombination was confirmed by Southern blotting. Two targeted clones (E142 and E147) were injected into C57BL/6 blastocysts and both produced germ-line chimeras. Chimeras were mated with C57BL/6 females, and their offspring were interbred. Heterozygous male mice were also bred with female *splicer* mice to delete the floxed neo cassette (Koni et al. 2001). Their offspring were screened for the targeted allele without the neo cassette and absence of the cre transgene. The resulting mouse lines were named E142/Neo$^-$ and E147/Neo$^-$. All further analyses were performed on a mixed (129 × C57BL/6) background. The four lines exhibited the same mutant phenotype.

To establish *Ecsit*$^{-/-}$ ES cell lines, *Ecsit*$^{+/-}$ mice were mated and blastocysts were collected, and ES cell lines were isolated from the inner cell mass grown in culture as described (Robertson 1987). The genotypes of ES cell lines were determined by Southern blotting.

Whole-mount in situ hybridization and TUNEL assays

Embryos were dissected free of maternal tissues, the Reichert's membrane removed, and fixed in 4% paraformaldehyde in PBS. Whole-mount in situ hybridization and TUNEL assay were performed as described (Sasaki and Hogan 1993; Conlon et al. 1995) with minor modifications. NBT-BCIP (Sigma) was used as the coloring reagent in the experiments presented in Figure 2C–F, whereas purple-precipitating reagent (Roche) was used in the other experiments. Normal and mutant embryos from the same mother were processed in the same well. A minimum of five mutant embryos were assessed for each probe at every developmental time point.

Histological analysis and immunofluorescence staining

Embryos within deciduas or teratomas were fixed overnight in 4% paraformaldehyde in PBS at 4°C, paraffin-embedded according to standard protocols, and sections (5 µm) were stained with hematoxylin and eosin. E6.5 and E7.5 embryos obtained from mating of heterozygotes were serially sectioned. Some sections from these embryos were hybridized with an *Ecsit2*-specific probe to identify *Ecsit*$^{-/-}$ mutant embryos.

For immunofluorescence staining, E6.75 embryos were serially sectioned, stained with rabbit anti-phospho-histone H3 (pH3) antibody (Upstate Biotechnology), and FITC-conjugated goat-anti-rabbit secondary antibody, followed by propidium iodide counterstaining. For quantification, all sections from two wild-type and two mutant embryos were stained, and pH3-positive cells were counted.

Growth analysis of ES cell lines

For growth analysis of ES cell lines, 5×10^4 ES cells were seeded in 60-mm tissue culture dishes with feeder cells or gelatin. Cells were suspended and counted every day for 4 d. Assays were done with two *Ecsit*$^{+/+}$, one *Ecsit*$^{+/-}$, and six *Ecsit*$^{-/-}$ ES clones; results from one *Ecsit*$^{+/+}$ clone and one *Ecsit*$^{-/-}$ clone are presented.

Generation of ES-cell-derived teratomas

To produce teratomas, 1×10^6 (Group A) or 2×10^6 (Group B) ES cells were injected subcutaneously into the flanks of CBy · Cg-Foxnl nu nude mice (Jackson Laboratory, Group A) or CD-1 nude mice (Charles River Laboratories, Group B). Each mouse was injected with wild-type ES cells on the left side and *Ecsit*$^{-/-}$ ES cells on the right side. Tumors were dissected 7 wk (Group A) or 9 wk (Group B) after injection. Teratomas were autopsied, weighed, and fixed overnight in 4% paraformaldehyde in PBS at 4°C. Histological analysis was performed as described above.

Generation and analysis of diploid aggregation chimeras

Chimeric embryos were generated by aggregation of *Ecsit*$^{+/+}$ and *Ecsit*$^{-/-}$ ES cells with ICR/Tg(ROSA26)/Rsor (Jackson Laboratories)-derived morulae as described (Hogan et al. 1994). Aggregates were implanted into recipient females, and the chimeric embryos were dissected at E8.5, E9.5, E12.5, and E14.5. Embryos were stained for β-galactosidase expression, fixed in formalin, and paraffin-sectioned. Sections were dewaxed and counterstained with Nuclear Fast Red.

Cell culture and transfection

P19 cells were maintained in MEM alpha medium (GIBCO) supplemented with 6% fetal bovine serum. Raw 264.7 and NIH/3T3 cells were maintained in DMEM (GIBCO) supplemented with 7% fetal bovine serum. Cells were transfected using Fugene 6 transfection reagent (Roche) following the manufacturer's instructions.

Generation of Ecsit *ShRNA*

Murine *Ecsit* target sequences (Sh1: GCTGTGGTTCACCC GATTC; Sh2: GGTCACTGTCTACCAGATG) were cloned into pSUPER.retro (OligoEngine) following the manufacturer's instructions. The EcoRI–XhoI cassette containing an H1-RNA promoter and ShRNA were excised and cloned into pBluescript KS+. The constructs were confirmed by DNA sequencing. To test ShRNAs, an expression vector encoding Flag-Ecsit2 and *Ecsit* ShRNAs were cotransfected into COS1 cells at 1:7 ratio. Then, 48 h after transfection, cells were lysed and whole cell lysates were immunoblotted with antibodies specific for Flag (Sigma) and GAPDH (Research Diagnostics, Inc.).

Reporter assays in P19, Raw 264.7, and NIH3T3

The Tlx2-Luc and pBIIx-Luc reporters have been described before (Zhong et al. 1997; Tang et al. 1998). The control plasmid used in transfection for luciferase assays was pBluescript KS+. A β-actin-Renilla luciferase plasmid was included to control transfection efficiency. Luciferase assays were carried out using the dual luciferase reporter assay system (Promega) and a Berthold luminometer. P19 cells were treated with 20 ng/mL Bmp4 (R&D Systems) as indicated, in media containing 0.2% serum for 15 h. Raw 264.7 cells were treated with 100 ng/mL LPS (Sigma) for 4 h, and NIH/3T3 cells were treated with 25 ng/mL TNFα (R&D Systems) for 4 h as indicated.

Immunoprecipitation assays

P19 cells were starved in Opti-MEM I (GIBCO) without serum for 15 h and then stimulated with 20 ng/mL Bmp4 (R&D Systems) for 30 min. Cells were washed once with ice-cold PBS and lysed in TNT Buffer (20 mM Tris-HCl at pH 8, 200 mM NaCl, 1% Triton X-100) with Complete Protease Inhibitor (Roche). The lysates were then subjected to immunoprecipitation using anti-Ecsit2 polyclonal antibody or its corresponding preimmune serum. A fraction of the lysates was subjected to direct immunoblotting to monitor the protein levels of Ecsit2, Smad1, and Smad4. Following SDS-PAGE electrophoresis, immunoprecipitated proteins were transferred to PVDF membranes (Immobilon-P, Millipore) and detected using antibodies specific for Smad4 (Santa Cruz Biotechnology) and Smad1 (Upstate Biotechnology).

Tlx2 *promoter analysis*

A series of 5′-end progressive deletions of the *Tlx2* promoter were generated using the Erase-a-Base System (Promega), based on the Tlx2-Luc (in pGL2-Basic Vector, Promega) plasmid (Tang et al. 1998). Another series of deletions spanning the Bmp-response element of the *Tlx2* promoter were generated by PCR and cloned into the pGL2-Promoter (Promega), which contained the SV40 promoter upstream of the luciferase gene. Promoter activity was analyzed by reporter assay in P19 cells as described above.

Chromatin immunoprecipitation

Analysis was performed following a kit protocol (Upstate Biotechnology). Chromatin from 2×10^6 P19 cells sheared using a Virtis Virsonic sonicator (4 × 10 sec; 1/10 power) was precleared with salmon sperm DNA-saturated protein A agarose, then precipitated using antibodies specific for Smad1, Smad4, Ecsit2, or beads alone. Samples were analyzed by PCR using HotStarTaq polymerase (QIAGEN) and primers for the *Tlx2* Bmp-response element (–1443/–1072; 5′-CGTGTCCAAGCCAGGCT GAGCA-3′, 5′-ACTTTACCCCACCCAAGCATCAG-3′), and a 3′-region of the *Tlx2* gene (4504/4759; 5′-CTGCCATTAAGC TAGGCTGG-3′, 5′-GCGCATGGTGTGCATAATAC-3′).

Acknowledgments

We thank Matthew Sarkisian, Crystal Bussey, Ken Harpal, Ingo von Both, and the Transgenic Mouse Facility at Mount Sinai Hospital for technical assistance; and Shannon T. Bailey for carefully reviewing our manuscript. This work was supported by grants from the NIH (R37-AI33443 to S.G.) and the Howard Hughes Medical Institute (S.G., R.A.F., and B.L.M.H.). M.K. was supported by a CIHR (Canadian Institutes of Health Research) postdoctoral fellowship. J.L.W. is a CIHR investigator and a Howard Hughes International Scholar.

The publication costs of this article were defrayed in part by payment of page charges. This article must therefore be hereby marked "advertisement" in accordance with 18 USC section 1734 solely to indicate this fact.

References

Aderem, A. and Ulevitch, R.J. 2000. Toll-like receptors in the induction of the innate immune response. *Nature* **406:** 782–787.

Beddington, R.S., Rashbass, P., and Wilson, V. 1992. Brachyury—A gene affecting mouse gastrulation and early organogenesis. *Development* **Suppl:** 157–165.

Bitzer, M., von Gersdorff, G., Liang, D., Dominguez-Rosales, A., Beg, A.A., Rojkind, M., and Bottinger, E.P. 2000. A mechanism of suppression of TGF-β/SMAD signaling by NF-κ B/RelA. *Genes & Dev.* **14:** 187–197.

Brummelkamp, T.R., Bernards, R., and Agami, R. 2002. A system for stable expression of short interfering RNAs in mammalian cells. *Science* **296:** 550–553.

Conlon, R.A., Reaume, A.G., and Rossant, J. 1995. Notch1 is required for the coordinate segmentation of somites. *Development* **121:** 1533–1545.

Coucouvanis, E. and Martin, G.R. 1999. BMP signaling plays a role in visceral endoderm differentiation and cavitation in the early mouse embryo. *Development* **126:** 535–546.

Deng, L., Wang, C., Spencer, E., Yang, L., Braun, A., You, J., Slaughter, C., Pickart, C., and Chen, Z.J. 2000. Activation of the IκB kinase complex by TRAF6 requires a dimeric ubiquitin-conjugating enzyme complex and a unique polyubiquitin chain. *Cell* **103:** 351–361.

Geiser, A.G., Letterio, J.J., Kulkarni, A.B., Karlsson, S., Roberts, A.B., and Sporn, M.B. 1993. Transforming growth factor β 1 (TGF-β 1) controls expression of major histocompatibility genes in the postnatal mouse: Aberrant histocompatibility antigen expression in the pathogenesis of the TGF-β 1 null mouse phenotype. *Proc. Natl. Acad. Sci.* **90:** 9944–9948.

Hata, A., Seoane, J., Lagna, G., Montalvo, E., Hemmati-Brivanlou, A., and Massague, J. 2000. OAZ uses distinct DNA- and protein-binding zinc fingers in separate BMP-Smad and Olf signaling pathways. *Cell* **100:** 229–240.

Hoffmann, J.A. and Reichhart, J.M. 2002. *Drosophila* innate immunity: An evolutionary perspective. *Nat. Immunol.* **3:** 121–126.

Hogan, B.L.M., Beddington, R., Costantini, F., and Lacy, E. 1994. *Manipulating the mouse embryo: A laboratory manual.* Cold Spring Harbor Laboratory Press, Cold Spring Harbor, NY.

Huang, J.D., Schwyter, D.H., Shirokawa, J.M., and Courey, A.J. 1993. The interplay between multiple enhancer and silencer elements defines the pattern of decapentaplegic expression. *Genes & Dev.* **7:** 694–704.

Koni, P.A., Joshi, S.K., Temann, U.A., Olson, D., Burkly, L., and Flavell, R.A. 2001. Conditional vascular cell adhesion molecule 1 deletion in mice: Impaired lymphocyte migration to bone marrow. *J. Exp. Med.* **193:** 741–754.

Kopp, E., Medzhitov, R., Carothers, J., Xiao, C., Douglas, I., Janeway, C.A., and Ghosh, S. 1999. ECSIT is an evolutionarily conserved intermediate in the Toll/IL-1 signal transduction pathway. *Genes & Dev.* **13:** 2059–2071.

Lawson, K.A., Dunn, N.R., Roelen, B.A., Zeinstra, L.M., Davis, A.M., Wright, C.V., Korving, J.P., and Hogan, B.L. 1999. Bmp4 is required for the generation of primordial germ cells in the mouse embryo. *Genes & Dev.* **13:** 424–436.

Letterio, J.J. and Roberts, A.B. 1997. TGF-β: A critical modulator of immune cell function. *Clin. Immunol. Immunopathol.* **84:** 244–250.

Lu, C.C., Brennan, J., and Robertson, E.J. 2001. From fertilization to gastrulation: Axis formation in the mouse embryo. *Curr. Opin. Genet. Dev.* **11:** 384–392.

McBurney, M.W. and Rogers, B.J. 1982. Isolation of male embryonal carcinoma cells and their chromosome replication patterns. *Dev. Biol.* **89:** 503–508.

Mishina, Y., Suzuki, A., Ueno, N., and Behringer, R.R. 1995. Bmpr encodes a type I bone morphogenetic protein receptor that is essential for gastrulation during mouse embryogenesis. *Genes & Dev.* **9:** 3027–3037.

Nichols, J., Zevnik, B., Anastassiadis, K., Niwa, H., Klewe-Nebenius, D., Chambers, I., Scholer, H., and Smith, A. 1998. Formation of pluripotent stem cells in the mammalian embryo depends on the POU transcription factor Oct4. *Cell* **95:** 379–391.

Power, M.A. and Tam, P.P. 1993. Onset of gastrulation, morphogenesis and somitogenesis in mouse embryos displaying compensatory growth. *Anat. Embryol. (Berl)* **187:** 493–504.

Rhinn, M., Dierich, A., Shawlot, W., Behringer, R.R., Le Meur, M., and Ang, S.L. 1998. Sequential roles for Otx2 in visceral endoderm and neuroectoderm for forebrain and midbrain induction and specification. *Development* **125:** 845–856.

Robertson, E.J. 1987. *Teratocarcinomas and embryonic stem cells: A practical approach.* IRL Press, Oxford, UK.

Rosner, M.H., Vigano, M.A., Ozato, K., Timmons, P.M., Poirier, F., Rigby, P.W., and Staudt, L.M. 1990. A POU-domain transcription factor in early stem cells and germ cells of the mammalian embryo. *Nature* **345:** 686–692.

Sanjo, H., Takeda, K., Tsujimura, T., Ninomiya-Tsuji, J., Matsumoto, K., and Akira, S. 2003. TAB2 is essential for prevention of apoptosis in fetal liver but not for interleukin-1 signaling. *Mol. Cell. Biol.* **23:** 1231–1238.

Sasaki, H. and Hogan, B.L. 1993. Differential expression of multiple fork head related genes during gastrulation and axial pattern formation in the mouse embryo. *Development* **118:** 47–59.

Shi, Y. and Massague, J. 2003. Mechanisms of TGF-β signaling from cell membrane to the nucleus. *Cell* **113:** 685–700.

Silver, D.P. and Livingston, D.M. 2001. Self-excising retroviral vectors encoding the Cre recombinase overcome Cre-mediated cellular toxicity. *Mol. Cell* **8:** 233–243.

Simeone, A., Acampora, D., Mallamaci, A., Stornaiuolo, A., D'Apice, M.R., Nigro, V., and Boncinelli, E. 1993. A vertebrate gene related to orthodenticle contains a homeodomain of the bicoid class and demarcates anterior neuroectoderm in the gastrulating mouse embryo. *EMBO J.* **12:** 2735–2747.

Stanley, E.G., Biben, C., Allison, J., Hartley, L., Wicks, I.P., Campbell, I.K., McKinley, M., Barnett, L., Koentgen, F., Robb, L., et al. 2000. Targeted insertion of a lacZ reporter gene into the mouse Cer1 locus reveals complex and dynamic expression during embryogenesis. *Genesis* **26:** 259–264.

Tang, S.J., Hoodless, P.A., Lu, Z., Breitman, M.L., McInnes, R.R., Wrana, J.L., and Buchwald, M. 1998. The Tlx-2 homeobox gene is a downstream target of BMP signalling and is required for mouse mesoderm development. *Development* **125:** 1877–1887.

Tremblay, K.D., Hoodless, P.A., Bikoff, E.K., and Robertson, E.J. 2000. Formation of the definitive endoderm in mouse is a Smad2-dependent process. *Development* **127:** 3079–3090.

Vidricaire, G., Jardine, K., and McBurney, M.W. 1994. Expression of the Brachyury gene during mesoderm development in differentiating embryonal carcinoma cell cultures. *Development* **120:** 115–122.

Vodovotz, Y., Geiser, A.G., Chesler, L., Letterio, J.J., Campbell, A., Lucia, M.S., Sporn, M.B., and Roberts, A.B. 1996. Spontaneously increased production of nitric oxide and aberrant expression of the inducible nitric oxide synthase in vivo in the transforming growth factor β 1 null mouse. *J. Exp. Med.* **183:** 2337–2342.

Wang, C., Deng, L., Hong, M., Akkaraju, G.R., Inoue, J., and Chen, Z.J. 2001. TAK1 is a ubiquitin-dependent kinase of MKK and IKK. *Nature* **412:** 346–351.

Wharton, K.A., Ray, R.P., and Gelbart, W.M. 1993. An activity gradient of decapentaplegic is necessary for the specification of dorsal pattern elements in the *Drosophila* embryo. *Development* **117:** 807–822.

Winnier, G., Blessing, M., Labosky, P.A., and Hogan, B.L. 1995. Bone morphogenetic protein-4 is required for mesoderm formation and patterning in the mouse. *Genes & Dev.* **9:** 2105–2116.

Wrana, J.L. 2000. Regulation of Smad activity. *Cell* **100:** 189–192.

Ying, Y. and Zhao, G.Q. 2001. Cooperation of endoderm-derived BMP2 and extraembryonic ectoderm-derived BMP4 in primordial germ cell generation in the mouse. *Dev Biol.* **232:** 484–492.

Zhong, H., SuYang, H., Erdjument-Bromage, H., Tempst, P., and Ghosh, S. 1997. The transcriptional activity of NF-κB is regulated by the IκB-associated PKAc subunit through a cyclic AMP-independent mechanism. *Cell* **89:** 413–424.